International Immunopharmacology 66 (2019) 260–266

Contents lists available at ScienceDirect

International Immunopharmacology

journal homepage: www.elsevier.com/locate/intimp

Apremilast ameliorates carfilzomib-induced pulmonary inflammation and vascular injuries

Faisal Imam[a,*], Naif O. Al-Harbi[a], Mohammed M. Al-Harbi[a], Wajhul Qamar[a,b], Khaldoon Aljerian[c], Osamah Mohammed Belali[a], Sary Alsanea[a], Ahmed Z. Alanazi[a], Khalid Alhazzani[a]

[a] Department of Pharmacology and Toxicology, College of Pharmacy, King Saud University, P.O. Box 2457, Riyadh 11451, Saudi Arabia
[b] Central Laboratory, Research Center, College of Pharmacy, King Saud University, P.O. Box 2457, Riyadh 11451, Saudi Arabia
[c] King Khalid University Hospital, College of Medicine, King Saud University, Forensic Medicine and Toxicology Unit, P.O. Box 2457, Riyadh 11451, Saudi Arabia

ARTICLE INFO

Keywords:
Carfilzomib
Acute lung injury
Apremilast
TNF-alpha
NF-kB

ABSTRACT

Acute lung injury (ALI) due to chemotherapy occurs frequently. It presents a challenge for clinicians managing therapies for different types of cancers. Carfilzomib (Kyprolis™) is a new proteasome inhibitor that shows promise for the treatment of relapsing multiple myeloma. However, several cases of severe ALI have raised concern about the use of carfilzomib against relapsed multiple myelomas. To improve the efficacy of carfilzomib, a new anti-inflammatory drug for psoriasis treatment, apremilast (Otezla™) was investigated for its protective effects against carfilzomib-induced ALI in rats. RT-PCR analyses revealed that carfilzomib administration in rats markedly increased the levels of tumor necrosis factor-alpha and nuclear factor-kappa B and myeloperoxidase activity with a concomitant increase in lipid peroxidation. The anti-inflammatory cytokine, interleukin-10, was downregulated following carfilzomib administration. Reduction in glutathione levels indicated diminished cellular antioxidant defenses in response to carfilzomib-induced ALI. ALI was confirmed by histopathological observations in lung tissue slices. Apremilast administration reduced lung inflammation in terms of reduction in myeloperoxidase activity and levels of tumor necrosis factor-alpha and alveolar infiltrating cells. Apremilast reversed all observed toxic effects of carfilzomib and prevented ALI in rats.

1. Introduction

Acute lung injury (ALI) as a toxic manifestation has a severe impact on health and can be life-threatening. Several chemotherapeutic drugs are acutely toxic to vital organs including the lungs [1–5]. Consequences of an acute lung event in patients receiving chemotherapy can be more severe considering their predisposing health condition. Carfilzomib (Kyprolis™) is a proteasome inhibitor that displayed promising clinical results and was approved by the Food and Drug Administration (FDA) in 2012 for the treatment of relapsing multiple myeloma [6]. However, severe to fatal lung injuries have been reported [7,8]. Siegel et al., in a grouped analyses, any grade of cardiac related adverse events reported are 22.1% (7.2% cardiac failure) and 69.0% for any respiratory related adverse events (42.2% dyspnea). More reports are needed to conclude something on the frequency of lung injuries by carfilzomib in humans [9]. Carfilzomib has also been reported to have cardiotoxic effects in patients [10,11]. Patients developed acute dyspnea about 2–3 h after the first dose of carfilzomib and chest X-ray showed a slight increase in pulmonary infiltration but fatal pulmonary hemorrhage occurs after the first dose of second cycle [12,13]. Other reported common side effects of carfilzomib include fatigue, nausea, anemia, and thrombocytopenia [14].

The large surface area and massive vasculature of the lungs leave this organ susceptible to various kinds of injuries. In most cases the response is elicited by a brisk inflammatory response. This is the reason why most debilitating lung diseases are inflammatory, including emphysema, bronchitis, bronchiolitis, asthma, fibrosis, and a collective form chronic obstructive pulmonary disease (COPD) [15].

Apremilast is a new anti-inflammatory drug that was recently approved by the FDA for the treatment of psoriasis and psoriatic arthritis [16–18]. It is a selective inhibitor of phosphodiesterase 4. Inhibition of this enzyme leads to increased levels of cyclic AMP, which results decreased production of proinflammatory cytokines, such as tumor necrosis factor-alpha (TNF-α), and an increase in anti-inflammatory cytokines including interleukin (IL)-10 [18].

The anti-inflammatory behavior made apremilast an intriguing

* Corresponding author.
E-mail address: fimam@ksu.edu.sa (F. Imam).

https://doi.org/10.1016/j.intimp.2018.11.023
Received 11 August 2018; Received in revised form 29 October 2018; Accepted 15 November 2018
Available online 28 November 2018

subject of study for the relief of ALI. In the present investigation, apremilast was chosen to see its effects against carfilzomib induced acute lung injury in rats.

2. Materials and methods

2.1. Chemicals and reagents

Carfilzomib and apremilast were purchased from Beijing Mesochem Technology Co., Ltd (Beijing, China). Myeloperoxidase (MPO), TNF-α, and Caspase-3 enzyme activity assay enzyme-linked immunosorbent assay (ELISA) kits were purchased from BioVision (Milpitas, CA, USA). Thiobarbituric acid (TBA) used for the malondialdehyde (MDA) assay and 5,5′-dithiobis (2-nitrobenzoic acid; DTNB, Ellman's reagent) for the glutathione (GSH) assay were purchased from Sigma Chemicals (St. Louis, MO, USA). Primers used for gene expression were purchased from Applied Biosystems (Paisley, UK) and Genscript (Piscataway, NJ, USA). High capacity cDNA reverse transcription kit and SYBER® green PCR Master Mix were also purchased from Applied Biosystems. TRIzol was purchased from Life Technology (Grand Island, NY, USA). Primary and secondary antibodies for protein expression were obtained from Santa Cruz Biotechnology (Dallas, TX, USA). Nitrocellulose membranes were purchased from Bio-Rad Laboratories (Hercules, CA, USA). Immobilon™ Western (chemiluminescent horseradish peroxidase (HRP) substrate) and western blot detection kits were obtained from Millipore Corporation (Billerica, MA, USA). Unless stated otherwise, all other chemicals used were of highest analytical grade and were purchased from Sigma Chemicals.

2.2. Animals and treatment regimen

Male albino rats approximately 8 weeks old and weighing 200–240 g were procured from the experimental animal care center, College of Pharmacy, King Saud University, Riyadh, Kingdom of Saudi Arabia. They were kept in controlled environmental conditions of temperature (22 ± 2 °C) and humidity (45–55%), and had free access to a standard pellet diet and fresh drinking water throughout the study. All experiments were carried out according to the Guidelines of Animal Care and Use Committee at King Saud University.

The rats were randomly divided into four groups. Group 1 was the control group, in which rats received normal saline for three weeks. Group 2 was the toxic group, in which rats received carfilzomib 4 mg/kg, intraperitoneally twice weekly for three consecutive weeks. Groups 3 and 4 were the treatment groups, with carfilzomib used following the same schedule as in group 2 plus apremilast administered orally at either 10 mg/kg/day (group 3) or 20 mg/kg/day (group 4) for three weeks.

2.3. Western blot analysis

Protein was extracted from lung tissue using protein lysis buffer as detailed previously [19]. Briefly, lung tissue was washed with ice-cold phosphate buffered saline, cut into small pieces, and homogenized separately in cold protein lysis buffer containing protease inhibitor cocktail [20]. Total protein was obtained by incubating the cell lysates on ice for 1 h, with intermittent vortex mixing every 10 min, followed by centrifugation at 12,000 ×*g* for 10 min at 4 °C. Total protein was measured using the Lowry method [21]. Protein expression was measured by the western blot technique as previously described [20]. Briefly, 25–50 μg of protein from each group was separated by 10% sodium dodecyl sulfate-polyacrylamide gel electrophoresis (SDS-PAGE) and electrophoretically transferred to an Immun-Blot® LV PVDF membrane (Bio-Rad). Protein blots were blocked overnight at 4 °C, followed by incubation with primary antibodies against nitric oxide synthase-2 (NOS-2), IL-17, nuclear factor-kappa B (NF-kB) p65, and IkBa (all from Santa Cruz Biotechnology) and HRP-conjugated secondary antibodies at room temperature. Bands were visualized using the enhanced Chemiluminescent HRP substrate (Millipore) and quantified relative to β-actin bands using the ImageJ® imaging processing program (National Institutes of Health, Bethesda, MD, USA). Images were taken using a C-Digit Chemoluminescent Western blot scanner (LI-COR, Lincoln, NB, USA).

2.4. RT-PCR analysis

2.4.1. RNA extraction and cDNA synthesis

Crushed ice and ice-cold reagents were used for extraction of RNA and cDNA synthesis steps. Lungs tissue was homogenized with TRIzol reagents (Life Technology/Invitrogen, Carlsbad, CA, USA) to isolate total RNA as described by the manufacturer. Quantification of total isolated RNA was done by measuring absorbance at 260 nm and 280 nm and determining the 260/280 ratio. A ratio < 0.2 indicated pure RNA. High capacity cDNA and reverse transcription kit (Applied Biosystems) was used to convert 1 μg of total RNA into first strand cDNA, following the manufacturer's instructions. Briefly, from each sample of total RNA, 1.5 μg was added to a mixture of 2.0 μl of 10× reverse transcription buffer, 0.8 μl of 25× dNTP mix (100 mM), 2.0 μl of 10× reverse transcription random primers, 1.0 μl of Multi-scribe reverse transcriptase, and 3.2 μl of nuclease-free water. This reaction mixture was kept at 25 °C for 10 min and then heated to 37 °C for 120 min, followed by 85 °C for 5 min, and then cooled at 4 °C [20].

2.4.2. RT-PCR quantification of mRNA expression in lung tissue via RT-PCR

Quantitatively specific gene mRNA expression analysis was done by real-time polymerase chain reaction (RT-PCR) using 96-well reaction plate PCR amplifier in the Fast ABI 7500 sequence detection system (Applied Biosystems) as previously described [20] [2]. The 25 μl reaction mixture contained 0.1 μl of 10 μM forward and 0.1 μl of 10 μM reverse primer (40 μM final concentration of each primer), 12.5 μM of SYBER green Universal Master Mix, 11.05 μl of nuclease-free water, and 1.25 μl of cDNA sample. The primers were purchased from Integrated DNA Technology (Coralville, IA, USA). The sequences were selected from PubMed and our database (Table 1). The levels of target mRNA expression were expressed as the fold-change between the groups and were correlated by the levels of mRNA expression of β-actin. The RT-PCR data were analyzed using the relative gene expression (i.e., $\Delta\Delta C_T$) method [19].

2.5. MPO activity

MPO is associated with the induction of lung injury, which reflects

Table 1
Rat primers sequence used for RT-PCR reactions.

Gene	Forward primer	Reverse primer
TNF-α	5′GCGGAGTCCGGGCAGGTCTA3′	5′GGGGGCTGGCTCTGTGAGGA3′
IL-10	5′ACCTGCTCCACTGCCTTGCT3′	5′GGTTGCCAAGCCTTATCGGA3′
NF-kB	5′ACCCCTTTCAAGTTCCCATAGA3′	5′ACCTCAATGTCTTCTTTCTGCAC3′
β-Actin	5′CCAGATCATGTTTGAGACCTTCAA3′	5′GTGGTACGACCAGAGGCATACA3′

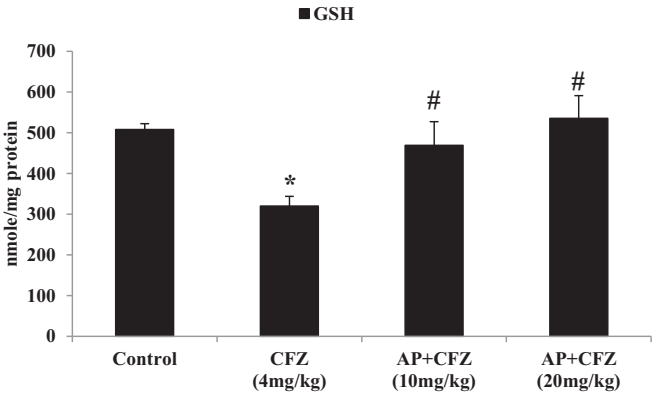

Fig. 1. Effects of apremilast on CFZ-induced decrease in glutathione content. Statistical analysis was performed using one-way ANOVA followed by Newman-Keuls Multiple comparisons test. *p < 0.05 compared with control group; #p < 0.05 compared with the carfilzomib group.

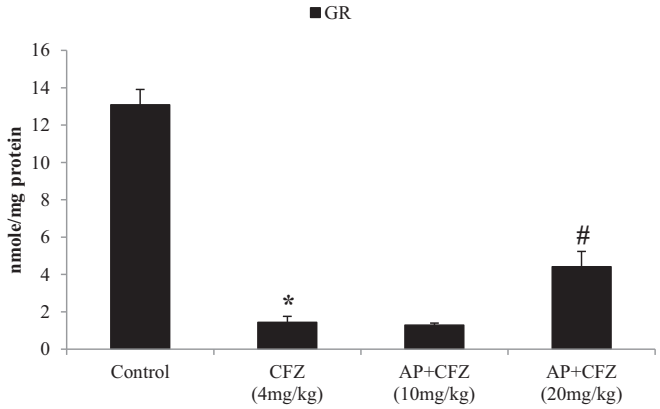

Fig. 2. Effects of apremilast on CFZ-induced decrease in glutathione reductase activity. Statistical analysis was performed using one-way ANOVA followed by Newman-Keuls Multiple comparisons test. *p < 0.05 compared with control group; #p < 0.05 compared with the carfilzomib group.

the infiltration of neutrophils into the lung. MPO activity was measured utilizing 3,3′,5,5′ tetramethylbenzidine (TMB) in 96-well microtitre plates in a modification of a previously described procedure [22]. Briefly, the reaction mixture containing MPO substrate buffer and the supernatant was incubated for 20 min at room temperature. The reaction mixture was assayed for MPO activity by measuring the optical density (OD) at 460 nm.

2.6. Determination of TNF-α

TNF-α in the lung tissue homogenates were estimated with corresponding ELISA kit according to the manufacturer's instructions (Bio Legend, Inc., San Diego, CA, USA).

2.7. Determination of MDA content

An elevated MDA content in tissue indicates an increased lipid peroxidation, which in turn indicates increased tissue/cellular stress [23]. An aliquot (100 µl) of phenazine ethyl sulfate solution was added to a reaction mixture containing 200 µl of 8.1% (w/v) SDS, 1.5 ml of 20% (v/v) acetic acid (pH 3.5), 1.5 ml of 0.8% (w/v) TBA, and 700 µl distilled water. The reaction mixture was boiled for 1 h at 90 ± 5 °C, cooled under a flow of tap water, centrifuged at 8000 × *g* for 10 min. The absorbance of the supernatant was measured using an ultraviolet (UV) spectrophotometer at 650 nm against a blank. MDA was expressed in nmol per mg protein.

2.8. Reduced GSH assay

The disparity in oxidant and antioxidant levels plays a significant role in lung inflammation. GSH levels in lung tissue were measured as previously described [24]. The absorbance of the reaction mixture was measured within 5 min of addition of DTNB at 412 nm using the UV spectrophotometer and compared against a blank.

2.9. GSH reductase (GR) activity

GR activity in lung tissue was measured as previously described [25] using a microplate reader. The absorbance of the sample and standard was measured at 412 nm at room temperature. The enzyme activity was expressed as nmol NADPH oxidized/min/mg protein.

2.10. Histopathological evaluation

Lung tissues were harvested on the final day of dosing, 4 h after p.o. administration of apremilast. Each tissue sample was fixed for 4 days in 10% buffer formosaline, decalcified in ethylenediamine tetraacetic acid in 5% formic acid, embedded in paraffin, and sectioned (3–4 µm). Tissue sections were stained with hematoxylin and eosin (H&E) for histopathological examination by light microscopy. Alveolar destruction, vascular proliferation, and inflammatory cell infiltration were assessed.

2.11. Statistical analyses

All data are presented as the mean ± SEM with six animals included in each group. One-way ANOVA was followed by Newman-Keuls Multiple comparison test. Data was considered statistically significant when the p-value was < 0.05. Statistical analysis was performed by using GraphPad Prism 3.0, (GraphPad Software, La Jolla, CA, USA).

3. Results

3.1. Endogenous antioxidant defenses

The administration of carfilzomib resulted in a marked decrease in GSH content and GR activity as compared to control (Figs. 1 and 2). Treatment with apremilast showed dose dependent effects and produced a significant (p < 0.05) dose dependently increase in GSH content whereas in GR activity only higher dose showed reversal of GR activity. These effects confirmed that apremilast prevented carfilzomib-induced lung injury in rats.

3.2. Oxidative damage and inflammation

Carfilzomib administration caused significant oxidative damage to the cell membrane in terms of significant (p < 0.05) increased levels of MDA (Fig. 3). The increased levels of MDA were dose dependently reversed by apremilast treatment. The observed increases in the level of proinflammatory cytokine TNF-α (Fig. 4) and MPO activity (Fig. 5) in the carfilzomib administration group indicated the induction of inflammation accompanied by oxidative damage. Increased levels of TNF-α dose dependently reversed by apremilast while MPO enzymes showed similar activity with both doses of apremilast treatment.

3.3. Gene expression analysis

These findings were further confirmed by RT-PCR analysis. TNF-α is a pro-inflammatory marker. Apremilast inhibits TNF-α mediated activation of NF-kB and oxidative stress and prevents lung injury and formation of reactive oxygen species (ROS). RT-PCR analysis revealed an

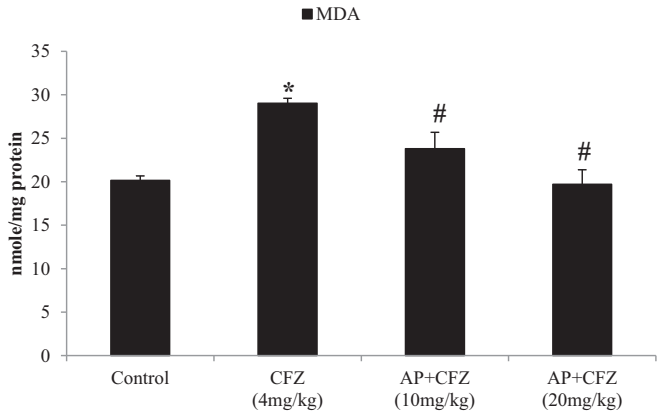

Fig. 3. Effects of apremilast on CFZ-induced increase in malondialdehyde levels. Statistical analysis was performed using one-way ANOVA followed by Newman-Keuls Multiple comparisons test. *p < 0.05 compared with control group; #p < 0.05 compared with the carfilzomib group.

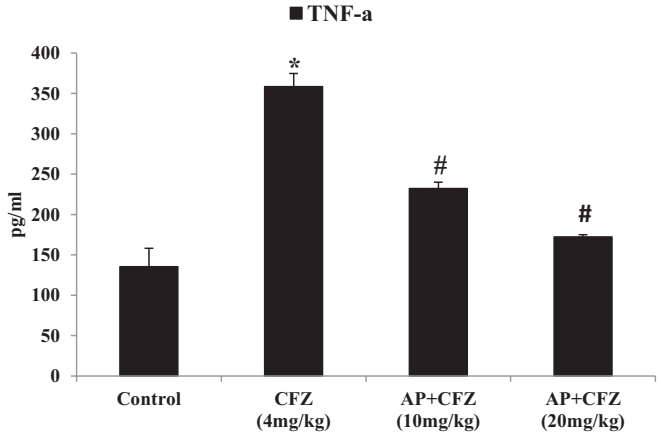

Fig. 4. Effects of apremilast on CFZ-induced increase in TNF-α levels. Statistical analysis was performed using one-way ANOVA followed by Newman-Keuls Multiple comparisons test. *p < 0.05 compared with control group; #p < 0.05 compared with the carfilzomib group.

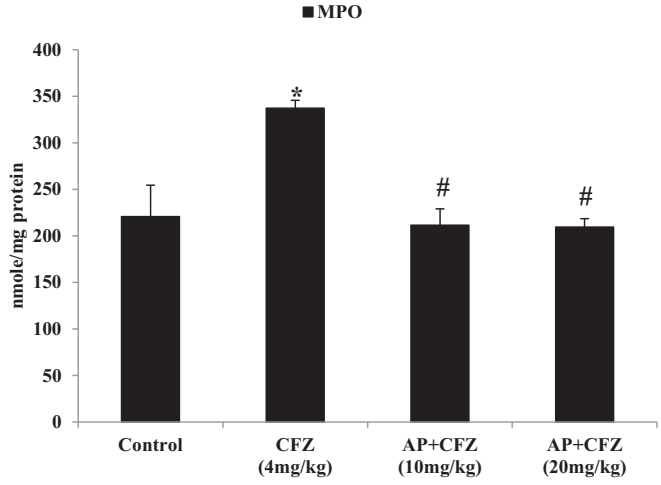

Fig. 5. Effects of apremilast on CFZ-induced increase in MPO activity. Statistical analysis was performed using one-way ANOVA followed by Newman-Keuls Multiple comparisons test. *p < 0.05 compared with control group; #p < 0.05 compared with the carfilzomib group.

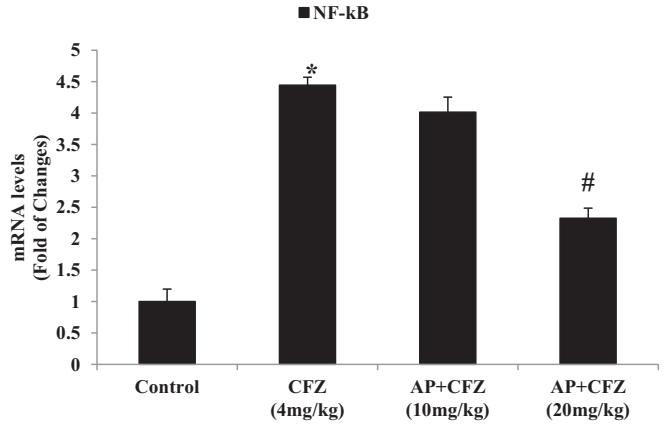

Fig. 6. Effects of apremilast on CFZ-induced increase in mRNA expression of NF-kB were measured by quantitative RT-PCR analysis. Each value indicates the mean ± SEM of six animals per group. Statistical analysis was performed using one-way ANOVA followed by the Newman-Keuls Multiple comparisons test. *p < 0.05 compared with control group; #p < 0.05 compared with the carfilzomib group.

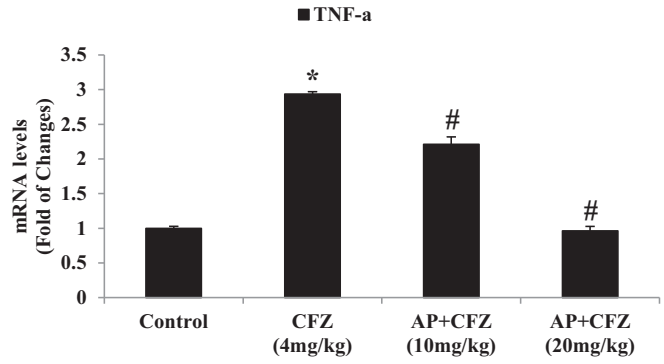

Fig. 7. Effects of apremilast on CFZ-induced increase in mRNA expression of TNF-α were measured by quantitative RT-PCR analysis. Each value indicates the mean ± SEM of six animals per group. Statistical analysis was performed using one-way ANOVA followed by the Newman-Keuls Multiple comparisons test. *p < 0.05 compared with control group; #p < 0.05 compared with the carfilzomib group.

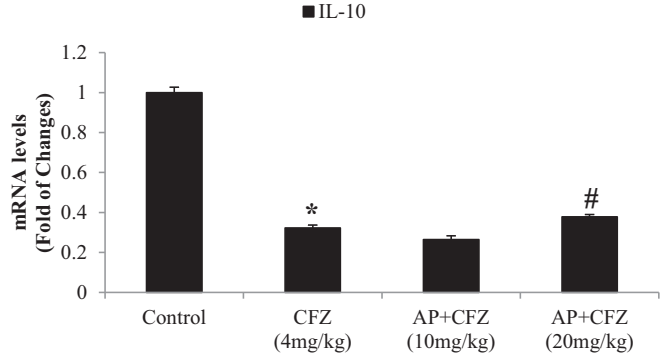

Fig. 8. Effects of apremilast on CFZ-induced decreased in mRNA expression of IL-10 were measured by quantitative RT-PCR analysis. Each value indicates the mean ± SEM of six animals per group. Statistical analysis was performed using one-way ANOVA followed by the Newman-Keuls Multiple comparisons test. *p < 0.05 compared with control group; #p < 0.05 compared with the carfilzomib group.

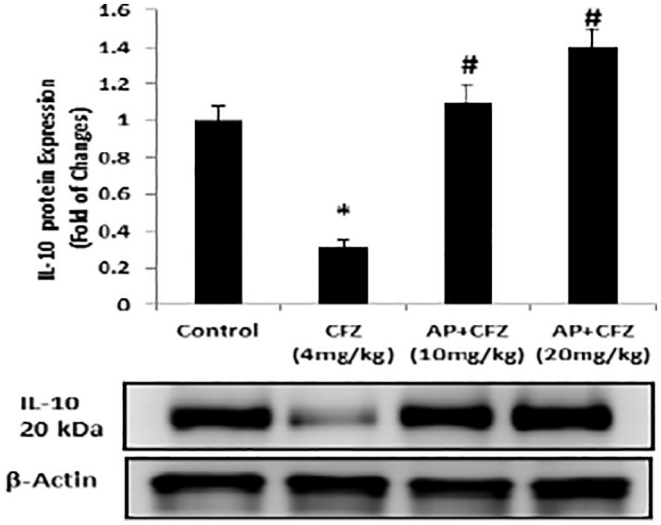

Fig. 9. Effects of apremilast on CFZ-induced decreased in expression of IL-10 protein were measured by western blot analysis. Statistical analysis was performed using one-way ANOVA followed by the Newman-Keuls Multiple comparisons test. *p < 0.05 compared with control group; #p < 0.05 compared with the carfilzomib group.

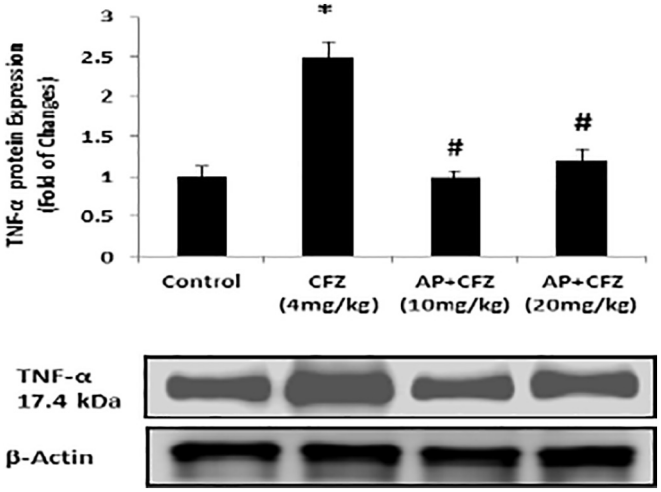

Fig. 10. Effects of apremilast on CFZ-induced decreased in expression of TNF-α protein were measured by western blot analysis. Statistical analysis was performed using one-way ANOVA followed by the Newman-Keuls Multiple comparisons test. *p < 0.05 compared with control group; #p < 0.05 compared with the carfilzomib group.

increased mRNA expression of TNF-α and NF-κB p65 in the carfilzomib group. These increases were reversed by treatment with apremilast in lung tissues (Figs. 6 and 7). Carfilzomib downregulated the expression of IL10, an anti-inflammatory cytokine (Fig. 8). The higher dose of apremilast (20 mg/kg) significantly reversed the effects on IL10. Effects on pro- and anti-inflammatory cytokines (TNF-α and IL10, respectively) were confirmed by western blot analysis (Figs. 9 and 10).

3.4. Histopathology

The histopathological data are presented in Fig. 11. The normal morphological structures were seen in the control groups (Fig. 11A and B), whereas innumerable histopathological degenerative changes were evident with carfilzomib treatment in lung tissue at 40× and 60× (Fig. 11C, D, E, F, G, H, I). Treatment of rats with carfilzomib produced severe vascular changes and hemorrhage, as evident by the presence of neutrophil in to the interstitial and alveolar spaces, macrophage and some eosinophils. Histological changes also shows presence of proteinaceous debris filled in the airspaces, hyalinization of the membranes and alveolar septal thickening. Infiltration of the neutrophils and monocytes in to the interstitial space, alveolar septal thickening and presence of hyaline membrane represents as pneumocyte injury. These changes were impeded by apremilast (Fig. 11J, K and L). Carfilzomib produced histopathological findings of microscopic hemorrhage (Fig. 11B, C). Vascular changes also identified (Fig. 11D & E), and included hyalinization, and endothelial and smooth muscle proliferation (Fig. 11D, E), plexiform vascular structures, and recanalization (Fig. 11H, I). Inflammatory infiltrate was predominantly drug-induced neutrophil and eosinophilic infiltrate. Additionally, there was infiltration of plasma cells, lymphocytes, and histiocytes. Hemorrhage was documented by identifying hemosiderin-laden macrophages, which showed refractile, coarse brown-colored pigment engulfed by macrophages (Fig. 11E, F). Treatment with apremilast markedly reduced infiltration of neutrophil in to the interstitial and alveolar spaces, macrophage and eosinophils. Significantly reduced membrane hyalinization and alveolar septal thickening. Treatment with apremilast reverses these changes but some scars of toxicity also reported. Scoring of lung injury were done using lung injury scoring system (Table 2) and a lung injury score data presented in Table 3.

4. Discussion

Chemotherapeutic interventions often have toxic effects on the cancerous cells and normal healthy cells as well. Usually, healthy dividing cells, including bone marrow, gastrointestinal mucosa, and hair follicles are the primary targets of the anticancer agents. However, these agents can also exert their toxic effects on particular organs, including the lung, liver, kidneys, and heart, among others. Carfilzomib, which is used in the treatment of relapsing multiple myeloma, also has toxic effects that include lung injury.

The present investigation focused on the inflammatory lung injury induced by carfilzomib in rats. The administration of carfilzomib induced lung inflammation that was evident by increased levels of the proinflammatory cytokine, TNF-α, and increased MPO activity. These effects were accompanied by depletion in cellular antioxidant defenses, as evident by reduced GSH and GR activities. The increase in lipid peroxidation emphasized the oxidative damage in the inflammatory environment. The oxidative environment plays a major role in inflammatory processes and induction of TNF-α [26]. Presently, these effects were efficiently reversed by the anti-inflammatory drug apremilast. These findings provide further evidence of the establishment of oxidative stress in an inflammatory environment, and not vice versa.

While the reversal of oxidative stress by apremilast was apparent, the inclusion of parameters associated with inflammation associated parameters means the findings do not conclusively suggest the apremilast has antioxidant activities. The findings do infer that the oxidative stress produced in the present experimental setup was a consequence of inflammation induced by carfilzomib.

The NF-κB pathway is activated by TNF-α and plays an important role in inflammation [27]. Another cytokine, IL10, is anti-inflammatory in nature [28] and plays a significant role in NF-κB pathway regulation by inhibiting its activities. IL-10 inhibits TNF-α-mediated NF-κB activation [29]. We observed that carfilzomib upregulated TNF-α and downregulated IL10 along with upregulation of NF-κB, suggesting that this pathway is involved in the induction of inflammation by this drug and consequent lung injury. However, apremilast reversed these effects by significantly upregulating IL10. However, the lower dose of apremilast (10 mg/kg) remained ineffective in mitigating inflammatory effects induced by carfilzomib. All these effects were confirmed via histological examination of lung sections from the different groups of rats and compared with sections from controls.

It can be suggested that inflammation, and not oxidative stress,

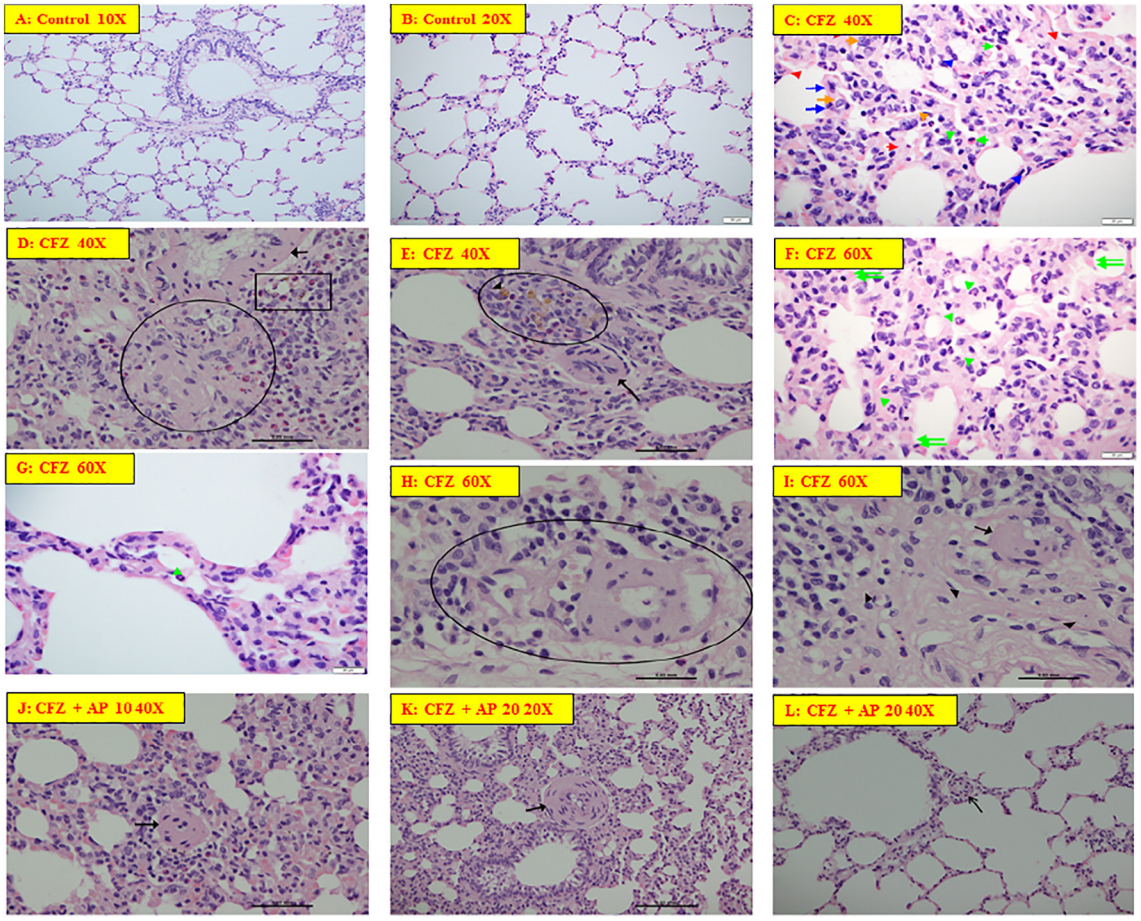

Fig. 11. (A & B): Showing normal morphological structures (H&E, 10× and 20× respectively).
C = Acute lung injury showing neutrophil in interstitial space (green arrowhead) and neutrophil in alveolar space (orange arrowhead) and some eosinophil (green arrow). Proteinaceous debris filling the airspaces (red arrow). Hyaline membranes (red arrowhead). Alveolar septal thickening (blue arrowhead). Macrophage (orange arrow) Pneumocyte injury (blue arrow).
D = Plexiform artery with slit like recanalization, hyalinization, endothelial & smooth muscle proliferation (circular). Hemorrhage and chronic inflammation (black rectangle). Endothelial and smooth muscle proliferation and hyalinization of pulmonary artery (black arrow).
E = Hemorrhage; refractile coarse brown pigment consistent with hemosiderin laden macrophages (black arrowhead). Chronic inflammation with neutrophils, histiocytes, plasma cells and lymphocytes (oval). Endothelial and smooth muscle proliferation and hyalinization of pulmonary artery (black arrow).
F = Neutrophil (green arrowhead) and pneumocyte injury (green double arrow).
G = Neutrophil (green arrowhead).
H = Plexiform artery with multiple slit like recanalization, hyalinization, endothelial & smooth muscle proliferation (oval). Also seen is chronic inflammation.
I = Plexiform artery with multiple slit like recanalization (arrowheads), hyalinization, endothelial & smooth muscle proliferation (arrow).
(J, K & L): Shows recovery from the toxicity but having some scars of toxicity. (For interpretation of the references to color in this figure legend, the reader is referred to the web version of this article.)

Table 2
Lung injury scoring system.

S. no	Parameter	Score per field		
		0	1	2
A.	Neutrophils in the alveolar space	None	1–5	> 5
B.	Neutrophils in the interstitial space	None	1–5	> 5
C.	Hyaline membranes	None	1	> 1
D.	Proteinaceous debris filling the airspaces	None	1	> 1
E.	Alveolar septal thickening	< 2×	2×–4×	> 4×

Score = [(20 × A) + (14 × B) + (7 × C) + (7 × D) + (2 × E)] / (number of fields × 100).

plays a central role in carfilzomib-induced lung injuries in rats, and that the anti-inflammatory agent apremilast is capable of preventing these injuries by inhibiting the NF-κB pathway by upregulating IL10 and downregulating TNF-α.

In the histopathological examination, inflammation, hemorrhage, and severe vascular changes (eosinophilic, plasmacytic, lymphocytic and histiocytic inflammation) were detected. These changes could be impeded by using 20 mg apremilast (Fig. 11A). Severe vascular changes, hemorrhage, and release of various inflammation mediators are characteristic features of ALI. Changes in the lung vasculature lead to pulmonary hemorrhage and inflammatory infiltrations [8,12,13,30]. Furthermore, this condition leads to hyalinization of the arterioles, endothelial and smooth muscle proliferation, plexiform vascular structures, and recanalization. These changes due to carfilzomib were reversed in a dose-dependent manner with apremilast. Carfilzomib additionally causes severe vasculopathy [11,30,31]. These findings are consistent with pulmonary hypertension [32–34]. Furthermore, carfilzomib induces lung inflammation, which we have demonstrated by carrying out histopathological studies, similar to a previous study [30].

In conclusion, the protective role of apremilast conveyed substantial attenuation of oxidative stress parameters, improvement in inflammatory markers, as well as restoration of lung structures. Thus, the current study suggests that apremilast may be beneficial in case of lung

Table 3
Histopathology scoring in lung injury.

S. no	Parameters	Control	CFZ (4 mg/kg)	AP + CFZ (10 mg/kg)	AP + CFZ (20 mg/kg)
A	Neutrophils in the alveolar space	0	2	1	0
B	Neutrophils in the interstitial space	0	2	1	1
C	Hyaline membranes	0	2	0	0
D	Proteinaceous debris filling the airspaces	0	2	1	1
E	Alveolar septal thickening	1	1	0	0
	Total score =	0.020	0.980	0.410	0.210

Note = Zero indicates no injury and one (1) indicates maximum injury.

injury caused by carfilzomib.

Treatment of rats with carfilzomib produced severe vascular changes and hemorrhage, indicated by neutrophil infiltration in to the interstitial space and alveolar spaces which were consistent with pulmonary hypertension and hemorrhage, and drug-related inflammation (eosinophilic, plasmacytic, lymphocytic and histiocytic inflammation).

Acknowledgments

The present study was funded by the Deanship of Scientific Research, King Saud University (Project No. RGP-VPP-305). The authors acknowledge the Department of Pharmacology and Toxicology, College of Pharmacy, King Saud University for its facilities.

Conflict of interest statement

There is no conflict of interest.

References

[1] R.M. Damiani, D.J. Moura, C.M. Viau, R.A. Caceres, J.A. Henriques, J. Saffi, Pathways of cardiac toxicity: comparison between chemotherapeutic drugs doxorubicin and mitoxantrone, Arch. Toxicol. 90 (9) (2016) 2063–2076, https://doi.org/10.1007/s00204-016-1759-y.
[2] A.H. Limper, Chemotherapy-induced lung disease, Clin. Chest Med. 25 (1) (2004) 53, https://doi.org/10.1016/S0272-5231(03)00123-0.
[3] M.A. Perazella, G.W. Moeckel, Nephrotoxicity from chemotherapeutic agents: clinical manifestations, pathobiology, and prevention/therapy, Semin. Nephrol. 30 (6) (2010) 570–581, https://doi.org/10.1016/j.semnephrol.2010.09.005.
[4] M. Schwaiblmair, W. Behr, T. Haeckel, B. Markl, W. Foerg, T. Berghaus, Drug induced interstitial lung disease, Open Respir. Med. J. 6 (2012) 63–74, https://doi.org/10.2174/1874306401206010063.
[5] C. Sioka, A.P. Kyritsis, Central and peripheral nervous system toxicity of common chemotherapeutic agents, Cancer Chemother. Pharmacol. 63 (5) (2009) 761–767, https://doi.org/10.1007/s00280-008-0876-6.
[6] G. Perel, J. Bliss, C.M. Thomas, Carfilzomib (Kyprolis): a novel proteasome inhibitor for relapsed and/or refractory multiple myeloma, Pharm. Ther. 41 (5) (2016) 303–307 Retrieved from http://www.ncbi.nlm.nih.gov/pubmed/27162470.
[7] A. Bhagavath, A. Geyer, Carfilzomib pulmonary toxicity, Chest 150 (4) (2016) 492a, https://doi.org/10.1016/j.chest.2016.08.506.
[8] A.R. Lataifeh, A. Nusair, Fatal pulmonary toxicity due to carfilzomib (Kyprolis™), J. Oncol. Pharm. Pract. 22 (5) (2016) 720–724, https://doi.org/10.1177/1078155215588630.
[9] D. Siegel, T. Martin, A. Nooka, R.D. Harvey, R. Vij, R. Niesvizky, A.Z. Badros, S. Jagannath, L. McCulloch, K. Rajangam, S. Lonial, Integrated safety profile of single-agent carfilzomib: experience from 526 patients enrolled in 4 phase II clinical studies, Haematologica 298 (11) (2013) 1753–1761.
[10] S. Atrash, A. Tullos, S. Panozzo, M. Bhutani, F. Van Rhee, B. Barlogie, S.Z. Usmani, Cardiac complications in relapsed and refractory multiple myeloma patients treated with carfilzomib, Blood Cancer J. 5 (2015) e272, https://doi.org/10.1038/bcj.2014.93.
[11] A. Chari, D. Hajje, Case series discussion of cardiac and vascular events following carfilzomib treatment: possible mechanism, screening, and monitoring, BMC Cancer 14 (2014) 915, https://doi.org/10.1186/1471-2407-14-915.
[12] Y.L. Kwong, Fatal pulmonary hemorrhage after carfilzomib treatment in multiple myeloma, Ann. Hematol. 94 (8) (2015) 1425.
[13] M. Wang, J. Cheng, Overview and management of cardiac and pulmonary adverse events in patients with relapsed and/or refractory multiple myeloma treated with single-agent carfilzomib, Oncology (Williston Park) 27 (3) (2013) 24–30 Retrieved from https://www.ncbi.nlm.nih.gov/pubmed/25184233.
[14] J.M. Steele, Carfilzomib: a new proteasome inhibitor for relapsed or refractory multiple myeloma, J. Oncol. Pharm. Pract. 19 (4) (2013) 348–354, https://doi.org/10.1177/1078155212470388.
[15] D. Hartl, S. Krauss-Etschmann, B. Koller, P.L. Hordijk, T.W. Kuijpers, F. Hoffmann, ... D. Roos, Infiltrated neutrophils acquire novel chemokine receptor expression and chemokine responsiveness in chronic inflammatory lung diseases, J. Immunol. 181 (11) (2008) 8053–8067, https://doi.org/10.4049/jimmunol.181.11.8053.
[16] Apremilast for psoriasis and psoriatic arthritis, Drug Ther. Bull. 53 (9) (2015) 105–108, https://doi.org/10.1136/dtb.2015.9.0352.
[17] G. Schett, Apremilast in psoriatic arthritis, Clin. Exp. Rheumatol. 33 (5) (2015) S98–S100 (Retrieved from < Go to ISI > ://WOS:000364357100021).
[18] T. Zerilli, E. Ocheretyaner, Apremilast (Otezla): a new oral treatment for adults with psoriasis and psoriatic arthritis, Pharm. Ther. 40 (8) (2015) 495–500 Retrieved from http://www.ncbi.nlm.nih.gov/pubmed/26236137.
[19] F. Imam, N.O. Al-Harbi, M.M. Al-Harbi, M.A. Ansari, K.M. Zoheir, M. Iqbal, ... S.F. Ahmad, Diosmin downregulates the expression of T cell receptors, pro-inflammatory cytokines and NF-kappaB activation against LPS-induced acute lung injury in mice, Pharmacol. Res. 102 (2015) 1–11, https://doi.org/10.1016/j.phrs.2015.09.001.
[20] F. Imam, N.O. Al-Harbi, M.M. Al-Harbia, H.M. Korashy, M.A. Ansari, M.M. Sayed-Ahmed, ... S. Bahashwan, Rutin attenuates carfilzomib-induced cardiotoxicity through inhibition of NF-kappaB, hypertrophic gene expression and oxidative stress, Cardiovasc. Toxicol. 17 (1) (2017) 58–66, https://doi.org/10.1007/s12012-015-9356-5.
[21] O.H. Lowry, N.J. Rosebrough, A.L. Farr, R.J. Randall, Protein measurement with the Folin phenol reagent, J. Biol. Chem. 193 (1) (1951) 265–275 Retrieved from http://www.ncbi.nlm.nih.gov/pubmed/14907713.
[22] K. Suzuki, H. Ota, S. Sasagawa, T. Sakatani, T. Fujikura, Assay method for myeloperoxidase in human polymorphonuclear leukocytes, Anal. Biochem. 132 (2) (1983) 345–352 Retrieved from http://www.ncbi.nlm.nih.gov/pubmed/6312841.
[23] F. Imam, N.O. Al-Harbi, M.M. Al-Harbi, M.A. Ansari, M.M. Almutairi, M. Alshammari, ... S.F. Ahmad, Apremilast reversed carfilzomib-induced cardiotoxicity through inhibition of oxidative stress, NF-kappaB and MAPK signaling in rats, Toxicol. Mech. Methods 26 (9) (2016) 700–708, https://doi.org/10.1080/15376516.2016.1236425.
[24] J. Sedlak, R.H. Lindsay, Estimation of total, protein-bound, and nonprotein sulfhydryl groups in tissue with Ellman's reagent, Anal. Biochem. 25 (1) (1968) 192–205 Retrieved from http://www.ncbi.nlm.nih.gov/pubmed/4973948.
[25] I. Carlberg, B. Mannervik, Purification and characterization of the flavoenzyme glutathione reductase from rat liver, J. Biol. Chem. 250 (14) (1975) 5475–5480 Retrieved from http://www.ncbi.nlm.nih.gov/pubmed/237922.
[26] S. Salzano, P. Checconi, E.M. Hanschmann, C.H. Lillig, L.D. Bowler, P. Chan, ... P. Ghezzi, Linkage of inflammation and oxidative stress via release of glutathionylated peroxiredoxin-2, which acts as a danger signal, Proc. Natl. Acad. Sci. U. S. A. 111 (33) (2014) 12157–12162, https://doi.org/10.1073/pnas.1401712111.
[27] T. Lawrence, The nuclear factor NF-kappaB pathway in inflammation, Cold Spring Harb. Perspect. Biol. 1 (6) (2009) a001651, https://doi.org/10.1101/cshperspect.a001651.
[28] S.S. Iyer, G. Cheng, Role of interleukin 10 transcriptional regulation in inflammation and autoimmune disease, Crit. Rev. Immunol. 32 (1) (2012) 23–63 Retrieved from http://www.ncbi.nlm.nih.gov/pubmed/22428854.
[29] F. Driessler, K. Venstrom, R. Sabat, K. Asadullah, A.J. Schottelius, Molecular mechanisms of interleukin-10-mediated inhibition of NF-kappaB activity: a role for p50, Clin. Exp. Immunol. 135 (1) (2004) 64–73 Retrieved from http://www.ncbi.nlm.nih.gov/pubmed/14678266.
[30] M. Wang, J. Cheng, Overview and management of cardiac and pulmonary adverse events in patients with relapsed and/or refractory multiple myeloma treated with single-agent carfilzomib, Oncology 27 (Suppl. 3) (2013) 24–30.
[31] L. Hobeika, S.E. Self, J.C.Q. Velez, Renal thrombotic microangiopathy and podocytopathy associated with the use of carfilzomib in a patient with multiple myeloma, BMC Nephrol. 15 (1) (2014) 156.
[32] C. Guignabert, P. Dorfmüller, Pathology and pathobiology of pulmonary hypertension, Seminars in Respiratory and Critical Care Medicine, vol. 38, no. 05, Thieme Medical Publishers, October 2017, pp. 571–584.
[33] R.M. Tuder, J.C. Marecki, A. Richter, I. Fijalkowska, S. Flores, Pathology of pulmonary hypertension, Clin. Chest Med. 28 (1) (2007) 23–42.
[34] R.M. Tuder, E. Stacher, J. Robinson, R. Kumar, B.B. Graham, Pathology of pulmonary hypertension, Clin. Chest Med. 34 (4) (2013) 639–650.